Acute downregulation of connexin43 at wound sites leads to a reduced inflammatory response, enhanced keratinocyte proliferation and wound fibroblast migration

Ryoichi Mori[1], Kieran T. Power[3,*], Chiuhui Mary Wang[3,*], Paul Martin[1,2] and David L. Becker[3,‡]

Departments of [1]Physiology and [2]Biochemistry, School of Medical Sciences, University of Bristol, University Walk, Bristol BS8 1TD, UK
[3]Department of Anatomy and Developmental Biology, University College of London, Gower Street, London, WC1E 6BT, UK

*These authors contributed equally
‡Author for correspondence (e-mail: d.becker@ucl.ac.uk)

Accepted 30 October 2006
Journal of Cell Science 119, 5193-5203 Published by The Company of Biologists 2006
doi:10.1242/jcs.03320

Summary

Experimental downregulation of connexin43 (Cx43) expression at skin wound sites appears to markedly improve the rate and quality of healing, but the underlying mechanisms are currently unknown. Here, we have compared physiological and cell biological aspects of the repair process with and without Cx43 antisense oligodeoxynucleotide treatment. Treated wounds exhibited accelerated skin healing with significantly increased keratinocyte and fibroblast proliferation and migration. In vitro knockdown of Cx43 in a fibroblast wound-healing model also resulted in significantly faster healing, associated with increased mRNA for TGF-β1, and collagen α1 and general collagen content at the wound site. Treated wounds showed enhanced formation of granulation tissue and maturation with more rapid angiogenesis, myofibroblast differentiation and wound contraction appeared to be advanced by 2-3 days. Recruitment of both neutrophils and macrophages was markedly reduced within treated wounds, concomitant with reduced leukocyte infiltration. In turn, mRNA levels of CC chemokine ligand 2 and TNF-α were reduced in the treated wound. These data suggest that, by reducing Cx43 protein with Cx43-specific antisense oligodeoxynucleotides at wound sites early in the skin healing process repair is enhanced, at least in part, by accelerating cell migration and proliferation, and by attenuating inflammation and the additional damage it can cause.

Key words: Connexin43, Gap junction, Wound healing, Inflammation, antisense

Introduction

Skin wounds repair by a combination of re-epithelializing action, connective tissue contraction and an angiogenic response which leads to a dense network of blood vessels in the wound granulation tissue (Grose and Werner, 2004; Martin, 1997). A robust inflammatory response commences soon after any tissue damage. This both protects the wound from microbial infection and produces bioactive substances that act at the wound site. A variety of inflammatory cells migrate into the wound fulfilling several different functions. Neutrophils are the earliest leukocytes to be recruited to the wound and their main role is to defend the host from invasion by microbes, which they do by releasing toxic free oxygen radicals and secreting proinflammatory cytokines. Subsequently, macrophages clear away spent neutrophils and other cell and extracellular matrix debris at the wound site. Macrophages are the major producers of cytokines, chemokines and growth factors that direct subsequent cell and tissue migration. Although many of the signals regulating the inflammation and tissue repair process are clearly diffusible and operate over long distances, local cell-cell communication via cell adhesion molecules and cell-cell junctions appears also to play a significant role.

One junctional link between cells that may play a significant regulatory role is the gap junction, a hexameric channel formed of proteins from the connexin family. Expressed by almost all cells in the body (Wei et al., 2004), they have been shown to mediate changes in cell migration (Huang et al., 1998; Bannerman et al., 2000; Kwak et al., 2001; Li et al., 2002), proliferation (Becker and Mobbs, 1999; Lucke et al., 1999), inflammation (Oviedo-Orta et al., 2000; Oviedo-Orta et al., 2001) and contraction (Bowman et al., 1998; Ehrlich and Rittenberg, 2000).

The level of connexin43 (Cx43) protein at the epidermal wound edge naturally decreases over 24-48 hours (Goliger and Paul, 1995; Coutinho et al., 2003). We have recently reported that actively downregulating Cx43 protein levels by application of antisense oligodeoxynucleotides (asODN) to skin wound and burn injury sites, leads to significantly accelerated healing compared with wounds treated with sense oligodeoxynucleotides (sODN; control) (Qiu et al., 2003; Coutinho et al., 2005). However, we know very little about the cellular mechanisms underlying this accelerated healing.

Here, we show that acute downregulation of Cx43 protein at the wound site leads to an increase in keratinocyte proliferation and migration, and in the rate at which fibroblasts migrate into

the wound and lay down collagen matrix. We observed a decrease in neutrophil infiltration and a concomitant reduction in CC chemokine ligand 2 (Ccl2) and cytokine tumor necrosis factor α (TNF-α) mRNA. Subsequently, we saw a reduced recruitment of macrophages perhaps as a consequence of damping down of the initial inflammatory response, which is known to have downstream effects on the ensuing healing process. Together these modified responses resulted in significantly improved wound healing.

Results

Downregulation of Cx43 at wound sites with Cx43-asODN

As previously reported, Cx43 was found to be predominantly expressed in the lower and middle spinous cell layers of the epidermis and in fibroblasts, blood vessels and dermal appendages of intact skin. Six hours after the injury Cx43 was expressed in hyperproliferative epidermis but began to be downregulated in the leading edge keratinocytes (Goliger and Paul, 1995; Coutinho et al., 2003). Delivery of Cx43-asODN from the time of injury markedly reduced protein levels of Cx43 in the epidermis and dermis within 2 hours of treatment (as revealed by immunohistochemistry) (Qiu et al., 2003). Such a rapid knockdown is possible because Cx43 protein is turned over rapidly, sometimes within 1.5-2 hours (Laird et al., 1991; Gaitta et al., 2002). To quantify the extent of Cx43 protein and mRNA knockdown and recovery after asODN treatment more precisely, we compared expression levels of Cx43 mRNA at treated and untreated wound sites by real-time PCR (RT-PCR; Fig. 1). One day after injury, expression of Cx43 mRNA at Cx43-asODN-treated wounds was significantly reduced by comparison with control sODN-treated wounds (2.95 versus 4.7 units, respectively, a 37% reduction; $P<0.05$). By 7 days after the injury, however, expression levels were similar in the two wound regimes (4.6 versus 5.2 units for asODN- and control sODN-treated, respectively). Immunostaining of wounds for Cx43 at 1 day, 2 days and 7 days after wounding revealed very low levels of Cx43 protein in the epidermis and dermis of the Cx43-asODN-treated wound edge at day 1 compared with controls (Fig. 1). By day 2, some Cx43 staining had returned to the dermis of the Cx43-asODN-treated wound but the level was still very low in the epidermis. By day 7, in agreement with the RT-PCR findings, there was no obvious difference in Cx43 staining between treated and untreated wounds. These results confirm that Cx43-asODN, when delivered by Pluronic gel, does indeed inhibit the expression of Cx43 mRNA at early time points after wounding.

Accelerated closure and increased proliferation in Cx43-asODN-treated wounds

All wounds were photographed macroscopically under the same conditions and their areas measured digitally. As we have reported previously (Qiu et al., 2003) Cx43-asODN-treated wounds were significantly smaller, drier and less inflamed, and closed faster than control wounds at days 1 and 2 (data not shown). By day 7, scabs covered the wounds and made it impossible to give accurate measurements of wound closure. Re-epithelialization from the wound edge commenced soon after injury in order to cover the denuded site. Cx43-asODN treatment of both excisional and incisional wounds results in wounds that re-epithelialise more rapidly than control ODN

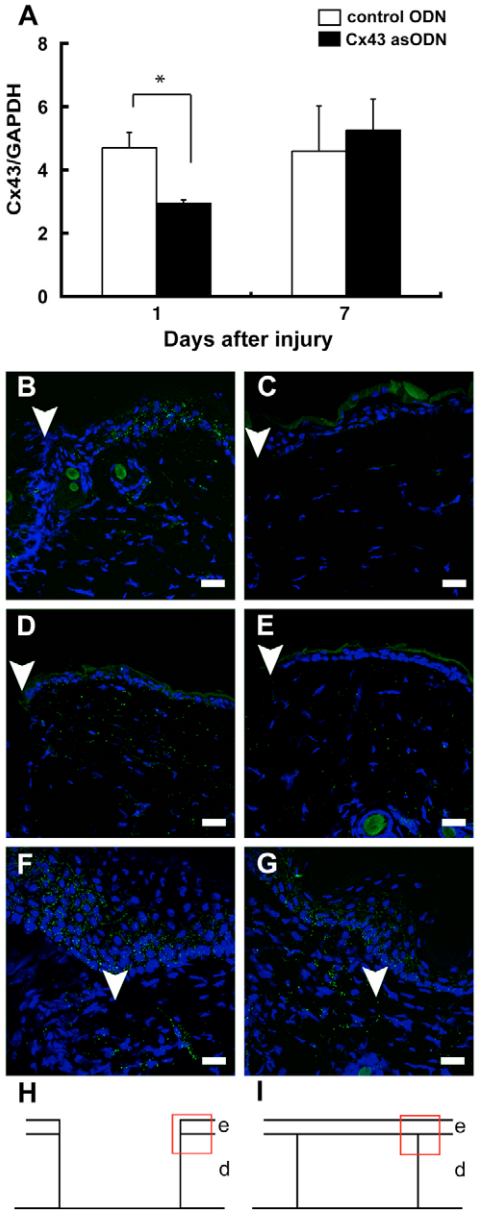

Fig. 1. Expression of Cx43 at wound sites. (A) Real-time PCR analysis of the gene expression of *Cx43* at wound sites. Relative expression levels of *Cx43* to GAPDH on days 1 and 7 in wounds treated with control sODN (n=4; white bars) and Cx43-asODN (n=4; black bars). Data are expressed as the mean ± s.e.m.; *$P<0.05$. (B-F) Cx43 staining (green) with bis-benzimide nuclear staining (blue) of control wounds (B, 1 day; D, 2 days; F, 7 days) or Cx43-asODN-treated wounds (C, 1 day; E, 2 days; G, 7 days). (H,I) Illustration of sites imaged in the wound edge. (H) Images B-E. (I) Images F and G. e, epidermis; d, dermis. For a high-resolution figure, please see the online version of this article.

treated wounds (Qiu et al., 2003). We therefore examined whether this is partially due to enhanced proliferation of keratinocytes and fibroblasts in the healing skin of Cx43-asODN-treated wounds (Fig. 2). Whereas there was little difference in keratinocyte proliferation between control and treated groups in the epidermal wound margin (Fig. 2E), we showed that, indeed, there are significantly increased numbers

of 5′-bromo-2′-deoxy-uridine (BrdU)-positive cells in the nascent epidermis of Cx43-asODN-treated wounds after both 2 days and 7 days (Fig. 2F). Similarly, counts of BrdU-positive cells in the dermal wound margin revealed slightly more cells following asODN-treatment and significantly more in the granulation tissue at days 1 and 2 (Fig. 2G,H). These results are consistent with our gross microscopic observations, and suggest that acute downregulation of Cx43 at wound sites leads to a surge of proliferation of wound-edge keratinocytes that continues as they re-epithelialize the wound. This enhanced proliferation might contribute to the accelerated re-epithelialization and enhanced granulation tissue maturation in asODN-treated wounds.

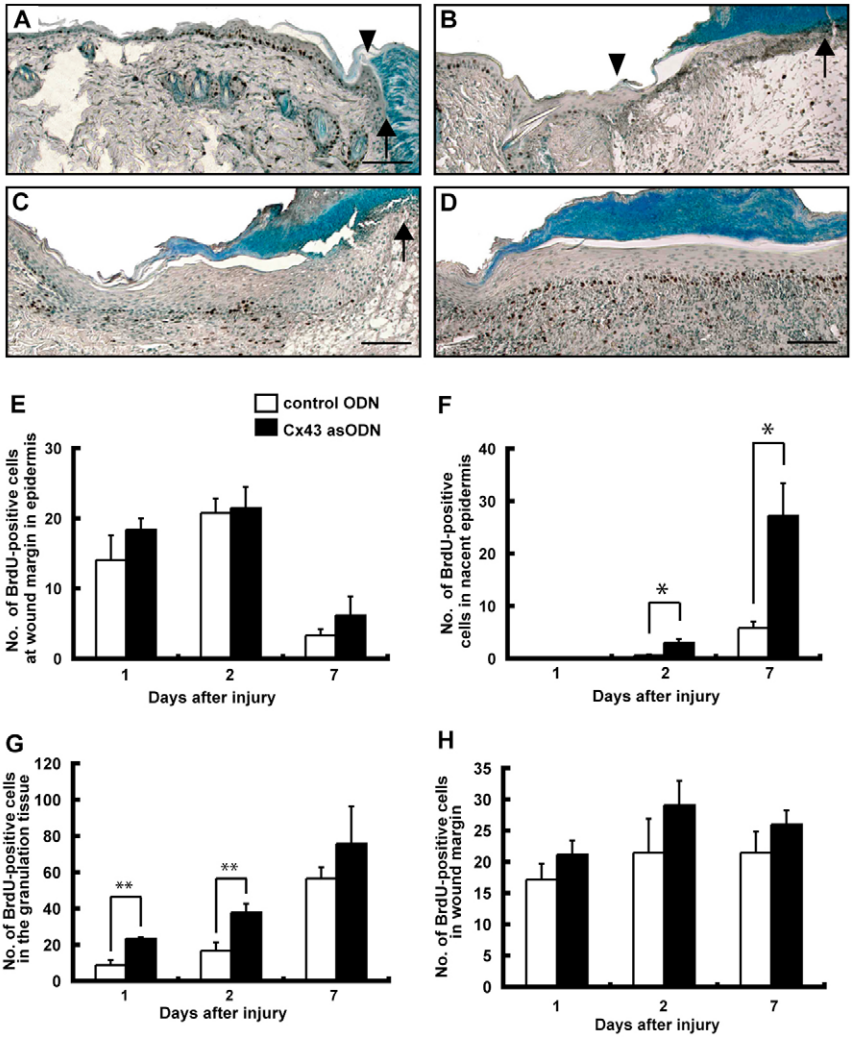

Fig. 2. Cell proliferation. (A-D) Analysis of cell proliferation at wound sites by immunohistochemical staining with the anti-BrdU monoclonal antibody in control ODN (A, day 2; C, day 7) and Cx43-asODN (B, day 2; D, day 7). Arrowhead and arrow indicate the wound margin and leading edge, respectively. (E,F) The number of BrdU-positive cells per field in the wound margin in the epidermis (E; n=5) and the nascent epidermis (F; n=5). (G,H) The number of BrdU-positive cells per 1.33 mm^2 in the dermal wound edge (G; n=5) and in the forming granulation tissue (H; n=5). Counts are expressed as the mean ± s.e.m.; *P<0.05. Bars, 200 μm.

Reduced influx of inflammatory cells in Cx43-asODN-treated wounds

Several leukocyte lineages infiltrate the wound site with varying time courses during the inflammatory response to tissue damage. The two primary cell lineages are neutrophils and macrophages, and both of these can exert profound effects on various aspects of the repair process. We have previously evaluated neutrophil influx in Cx43-asODN-treated wounds and here we confirm with an anti-myeloperoxidase (MPO) antibody that their numbers are significantly reduced on days 1 and 2, at a stage when neutrophil numbers are peaking in sODN-treated control wounds (Fig. 3). There is now clear evidence that the macrophage influx at a wound site may be linked to the rate of re-epithelialization and to the eventual extent of scarring at the wound site, so we have investigated macrophage numbers immunohistochemically by using F4/80 antibody against the marker of macrophage maturation and activation BM8 (Fig. 4). We found that the number of macrophages at Cx43-asODN-treated wound sites was significantly reduced at days 2 and 7 after the injury compared with control sODN-treated wounds, this being a reduction of 33% on day 2 and 32% on day 7 (Fig. 4C). These data clearly indicate that acute knockdown of Cx43 at the time of wounding leads to a dramatic subsequent reduction in both the early neutrophil and later, macrophage, inflammatory phases.

Reduced expression of Ccl2 and TNF-α in Cx43-asODN-treated wounds

Neutrophils and macrophages at the wound site release a large variety of proinflammatory cytokines and chemokines that act directly on cells in that site (keratinocytes, fibroblasts and endothelial cells) and amplify the wound inflammatory response. To examine how the reduced influx of inflammatory cells, after Cx43 knockdown, influences the level of these signals, we analyzed Ccl2 and TNF-α as a representative chemokine and cytokine, respectively. To quantify expression levels of Ccl2 and TNF-α we performed RT-PCR analysis on wound tissue on days 1, 2 and 7 (Fig. 5). Both mRNAs were robustly upregulated in control sODN-treated wound sites on day 1, and both peaked in expression levels at day 2, after which their levels decreased. By comparison, expression levels of Ccl2 and TNF-α in Cx43-asODN-treated wounds were significantly reduced (P<0.05) on day 2 (Ccl2) and 7 (TNF-α). These results indicate that reduced recruitment of neutrophils and macrophages in Cx43-asODN-treated wounds was indeed accompanied by diminished expression of these signaling molecules without compensation by other cell types.

Increased TGF-β1 expression at Cx43-asODN-treated wound sites

The wound-associated growth factor TGF-β1 plays a wide

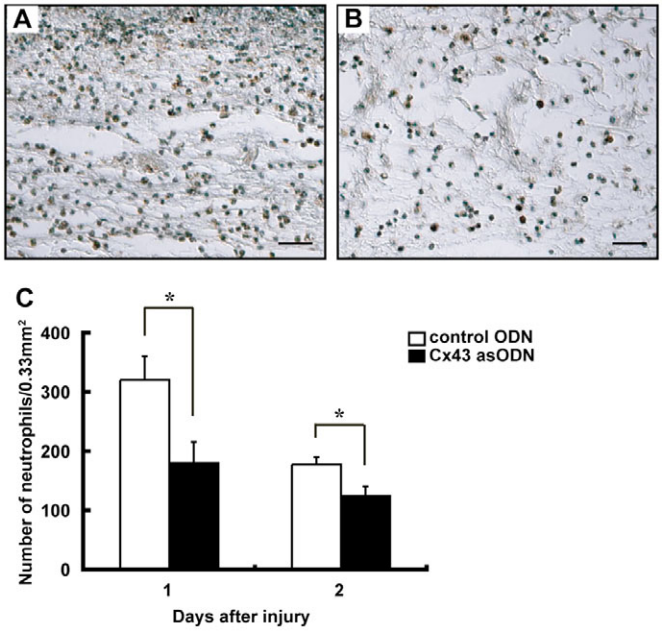

Fig. 3. Neutrophil recruitment into the wound site. (A,B) Neutrophil recruitment into skin wounds treated with control sODN (A) and Cx43-asODN (B), analyzed using an anti-MPO antibody on day 1. (C) Numbers of MPO-positive cells per 0.332 mm^2 at the wound site after treatment with control sODN (white bars: n=4 on day 1; n=5 on day 2) and Cx43-asODN (black bars; n=3 on day 1; n=4 on day 2). Data are expressed as the mean ± s.e.m. *P<0.05. Bars, 50 μm.

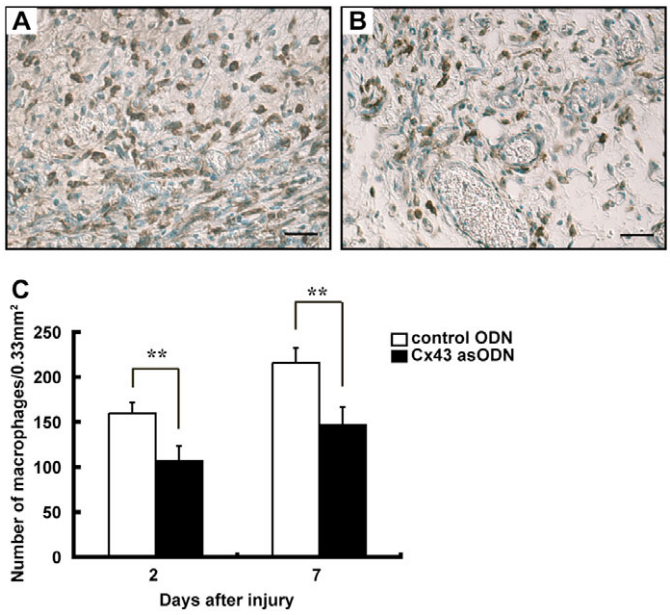

Fig. 4. Macrophage recruitment into the wound site. (A,B) Macrophage recruitment into skin wounds treated with control sODN (A) and Cx43-asODN (B), analyzed using an anti-F4/80 antibody on day 7. (C) Macrophage recruitment into skin wounds, cells per 0.332 mm^2 on days 2 and 7 after treatment with control sODN (white bars: n=4 on day 2, n=7 on day 7) and Cx43-asODN (black bars: n=4 on day 2, n=6 on day 7). Data are expressed as the mean ± s.e.m.; **P<0.01. Bars, 50 μm.

variety of roles at many stages of the wound-healing process. Therefore, we analyzed the expression levels of TGF-β1 at control sODN- and Cx43-asODN-treated wound sites with RT-PCR at 1 day, 2 days and 7 days after wounding (Fig. 6). TGF-β1 was at low levels on days 1 and 7 with no difference between control and treated wounds. However, on day 2 after the injury, the expression of TGF-β1 in asODN-treated wounds was significantly increased compared with control sODN-treated wounds (P<0.05). Immunostaining for TGF-β1 at day 2 revealed TGF-β1-positive cells in the dermis both at the wound site and in the adjacent tissues. Most of the cells were round and had the appearance of leucocytes. However, in the Cx43-asODN-treated tissue an additional TGF-β1-positive cell type could be seen in large numbers at the dermal margins of the wound. These cells appeared to be elongated and more fibroblast-like in their morphology. Interestingly, in the epidermis of Cx43-asODNs-treated wounds TGF-β1 appeared to stain much more strongly than in control-wound epidermis (Fig. 6). These results raise the possibility that increased expression of TGF-β1 might contribute to some of the changes we see in wound healing following Cx43-asODN treatment.

Granulation tissue formation and maturation

Connective-tissue wound contraction is a key component of the skin repair process. This step is closely associated with migration of fibroblasts into the wound bed and their differentiation into contractile myofibroblasts followed by their loss (Martin, 1997). Using Rhodamine-phalloidin combined with DAPI nuclear counter stain, we found a significant increase (mean of 39.4 in control and 99.2 in asODN-treated wounds; P<0.01) in the number of elongated fibroblast-like cells at the margin of 2-day-old Cx43-asODN-treated wounds compared with control wounds (Fig. 7A and B). These data suggest that the influx of fibroblasts to form wound granulation tissue is enhanced in wounds when Cx43 protein has been reduced. This may be due to both enhanced migration and the significantly greater cell proliferation that we see in the granulation tissue of asODN-treated wounds.

To investigate whether the enhanced rate of fibroblast migration was due to a reduction in Cx43 protein expression we used a fibroblast wound-healing assay. We knocked down Cx43 protein by applying Cx43-asODNs to confluent cultures of fibroblasts 2 hours prior to a scrape-wound assay. Because Cx43 protein is rapidly turned over (with a half life as short as 1.5-2 hours) this is sufficient to produce a significant knockdown of the protein within 2 hours (Fig. 7H,I), which can last between 8 and 48 hours depending on the cell type (Qiu et al., 2003; Pearson et al., 2005; Cronin et al., 2006). Fibroblast cultures that were treated with the Cx43-asODNs exhibited a significantly enhanced rate of wound closure compared with controls (Fig. 7F; P=0.02), which is entirely consistent with our in vivo findings. This strongly suggests that knockdown of Cx43 protein enhances the rate of migration of fibroblasts both in vitro and in vivo, and thereby promotes the rate of granulation tissue formation.

To investigate whether faster infiltration of fibroblasts leads to more rapid granulation tissue formation and alters the rate at which new collagen matrix is laid down, we measured the hydroxyproline (HP) content at the wound site. We found that HP content was significantly increased by day 7 in Cx43-

asODN-treated wounds when compared with control sODN-treated wounds (P<0.05), but thereafter HP content was similar in control and asODN-treated wounds (Fig. 8A). In accordance with this finding, the expression of mRNA for collagen type 1 α1 (Col1α1) was also significantly increased on day 2 and day 7 in Cx43-asODN-treated wounds compared with control-treated wounds (Fig. 8B; P<0.05).

When measuring granulation tissue areas, we found that treated tissue was slightly smaller than untreated tissue at day 5, but this difference was not significant. However, we found that on days 7, 10 and 14 after wounding Cx43-asODN-treated wounds exhibit significantly smaller areas of granulation tissue than control sODN-treated wounds (Fig. 9; *P<0.05, **P<0.01). To investigate how the more rapid contraction of the granulation tissue was brought about we stained sections by using a TUNEL labeling kit to look for apoptotic cell death, or with antibody against α smooth muscle actin (α-SMA), a marker of myofibroblasts. Although there were always slightly fewer apoptotic cells in treated granulation tissue, we found no significant differences in the numbers of TUNEL-positive cells between control and treated animals at 5, 7 and 10 days after wounding (Fig. 10). However, we observed a highly significant difference in the expression of α-SMA staining between the two groups at all of these time points (Fig. 11). At day 5, staining for α-SMA could be detected at the edges of the granulation tissue of Cx43-asODN-treated wounds but no staining was seen in control wounds. By day 7, staining for α-SMA could be detected at the edges of the granulation tissue of control wounds and throughout the granulation tissue of Cx43-asODN-treated wounds (Fig. 11A,B). Quantification of the staining at the edges of the granulation tissue revealed that it was significantly higher in Cx43-asODN-treated wounds (Fig. 11E; P=0.004). At 10 days after wounding most of the staining for α-SMA had gone from the edges of the granulation tissue of Cx43-asODN-treated wounds – with just a little remaining in the center of the wound. This was significantly different from control wounds, which showed strong α-SMA expression throughout the granulation tissue (Fig. 11C,D; P=0.000002). These findings imply that differentiation of fibroblasts into myofibroblasts occurs earlier in Cx43-asODN-treated wounds, and that these cells go on to contract the wound and are lost much faster than in control wounds. It would appear that Cx43-asODN-treated wounds are 2-3 days more advanced than controls in the maturation of their granulation tissue.

Angiogenesis

Besides the influx of fibroblasts, the other major cellular components of wound granulation tissue are the endothelial cells of new blood vessels. We therefore performed immunohistochemical staining using antibodies against CD31 and von Willebrand factor or FITC-labeled isolectin B in order to evaluate angiogenesis at treated wound sites at 5, 7, 10 and 14 days after wounding (Fig. 12). At 5 days, no blood vessel staining could be seen in the granulation tissue of control wounds, whereas staining was seen in the edges of the granulation tissue of all Cx43-asODN-treated wounds. At day 7, fine blood vessels were found throughout the entire granulation tissue in five out of six Cx43-asODN-treated wounds, but they had only just started to enter the edges of the granulation tissue of controls. However, whereas the blood

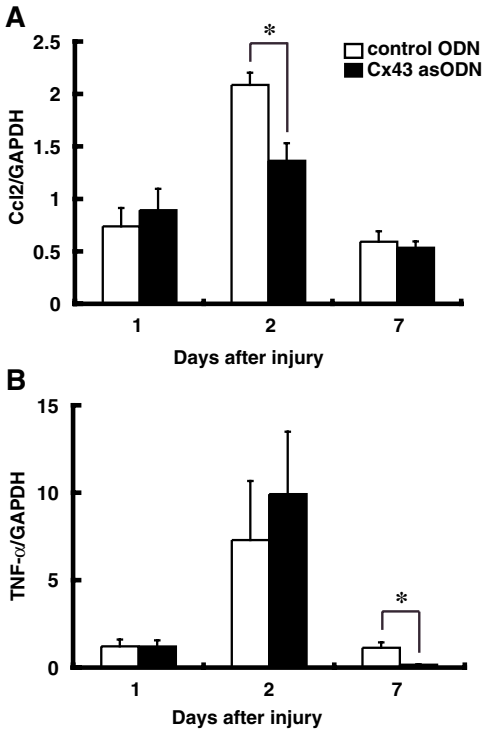

Fig. 5. Expression of Ccl2 and TNF-α at wound sites. (A,B) Real-time PCR analysis of the gene expression of *Ccl2* and TNF-α at wound sites. Relative expression levels of *Ccl2* (A) and TNF-α (B) to GAPDH on days 1, 2 and 7 (n=5 for each) after treatment with control sODN (white bars) or Cx43-asODN (black bars). Data are expressed as the mean ± s.e.m.; *P<0.05.

vessels of asODN-treated wounds were more pervasive they appeared to be significantly smaller or thinner than those of controls at this time point (Fig. 12B). This meant that, when blood vessel staining was quantified at 7 and 10 days there was significantly more staining in controls (7 days, P=0.0019; 10 days, P=0.015) where the vessels were bigger. At 14 days, the size of blood vessels and extent of staining were very similar in both treated and control groups (Fig. 12E,F). These findings suggest that angiogenesis takes place much earlier after Cx43-asODN treatment. Taken with our other findings relating to granulation tissue maturation it would seem that the treatment enhances the rate of wound maturation by 2-3 days.

Discussion

Cx43-asODN treatment rapidly downregulates Cx43 protein in the wound-site epidermis and dermis for at least 24 hours with some return of dermal expression by 48 hours and no obvious differences in Cx43 between groups after 7 days. Treatment leads to markedly accelerated skin wound healing, coincident with reduced leukocyte infiltration, reduced cytokines, increased re-epithelialization and enhanced wound contraction.

Inflammation

The initial response to wounding is typically the formation of a blood clot, which – together with local damaged tissue – releases proinflammatory signals, which trigger inflammatory cell infiltration in the form of neutrophils and then macrophages into the wound site. These signals and those

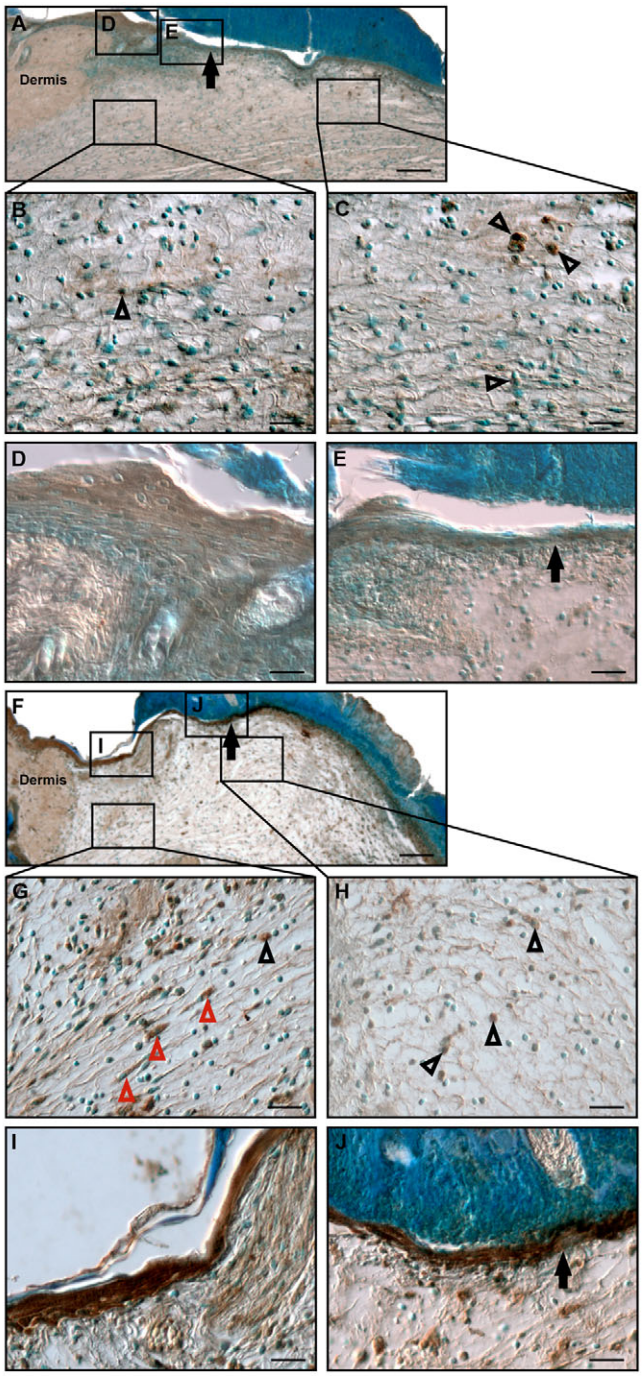

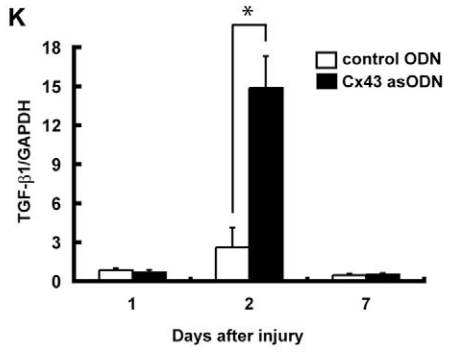

from the invading inflammatory cells influence both re-epithelialisation and connective tissue contraction of the wound (Martin, 1997). The migration of inflammatory cells into the wound is associated with cell-cell and cell-matrix interactions and with vasodilation of blood vessels. Cx43 is expressed in activated leukocytes, and at leukocyte-leukocyte and leukocyte-endothelial-cell contact sites during their extravasation under inflammatory conditions, and functional Cx43 channels are involved in release of cytokines and immunoglobulins (Oviedo-Orta and Evans, 2004). Numbers of neutrophils and macrophages were significantly reduced in Cx43-asODN-treated wounds, which is in keeping with the requirement for Cx43 expression for neutrophil extravasation and release of proinflammatory cytokines. The chemokine Ccl2 and cytokine TNF-α, which are chemoattractants for neutrophils and monocytes/macrophages (Rossi and Zlotnik, 2000), are also both reduced after Cx43-asODN treatment on day 2 and 7, respectively. Clearly, the reduced levels of these and other growth factors and cytokines at the wound site will have been both consequences of, and perhaps partial cause of, the reduced influx of neutrophils and other inflammatory cells.

Several recent reports have shown that a normal inflammatory response is not essential for skin wound healing (Martin and Leibovich, 2005). PU.1 null mice, which are genetically missing neutrophils and macrophages, repair skin lesions without scarring and at a similar rate to, or faster than, their wild-type siblings (Martin et al., 2003). Similarly, decreasing the numbers of neutrophils at wound sites by applying neutrophil antiserum leads to faster re-epithelialization (Dovi et al., 2003). What we cannot decipher from the current study is how much of the increase in epidermal migration and proliferative capacity is independent of the reduced inflammatory response and is, rather, a direct consequence of Cx43 knockdown in the leading-edge keratinocytes and fibroblasts. It is also unclear precisely how Cx43 knockdown leads to reduced leukocyte influx. The target tissue for Cx43-asODN action may be endothelial cells or leukocytes, both of which require Cx43 expression for effective extravasation and a robust inflammatory response (Oviedo-Orta et al., 2000; Oviedo-Orta et al., 2001). How Cx43 protein expression in endothelial cells or leukocytes regulates the inflammatory response is the subject of current investigations.

TGF-β1

In Cx43-asODN-treated wounds mRNA for TGF-β1 is significantly increased on day 2 compared with controls but is at relatively low levels in both treated and control wounds on day 1 and day 7. Expression of TGF-β1 is associated with

Fig. 6. Expression of TGF-β1. (A-J) Immunohistochemistry for TGF-β1 at wound sites treated with control sODN (A-E) and Cx43-asODN (F-J). Bars, 200 μm (A,F) and 50 μm (B-E,G-J). Black arrows show the nascent edge of the epidermis. TGF-β1 staining is considerably stronger in the epidermis of wounds treated with Cx43-asODN (I,J) compared with those treated with control sODN (D,E). Red and black arrowheads indicate representative TGF-β1-elongated fibroblast-like cells and rounded presumptive leukocytes, respectively. (K) Real-time PCR analysis of the expression on days 1, 2 and 7 (n=5 for each) of mRNA for TGF-β1 at wound sites treated with control sODN (white bars) or Cx43-asODN (black bars). Data are expressed as the mean ± s.e.m.; *P<0.05.

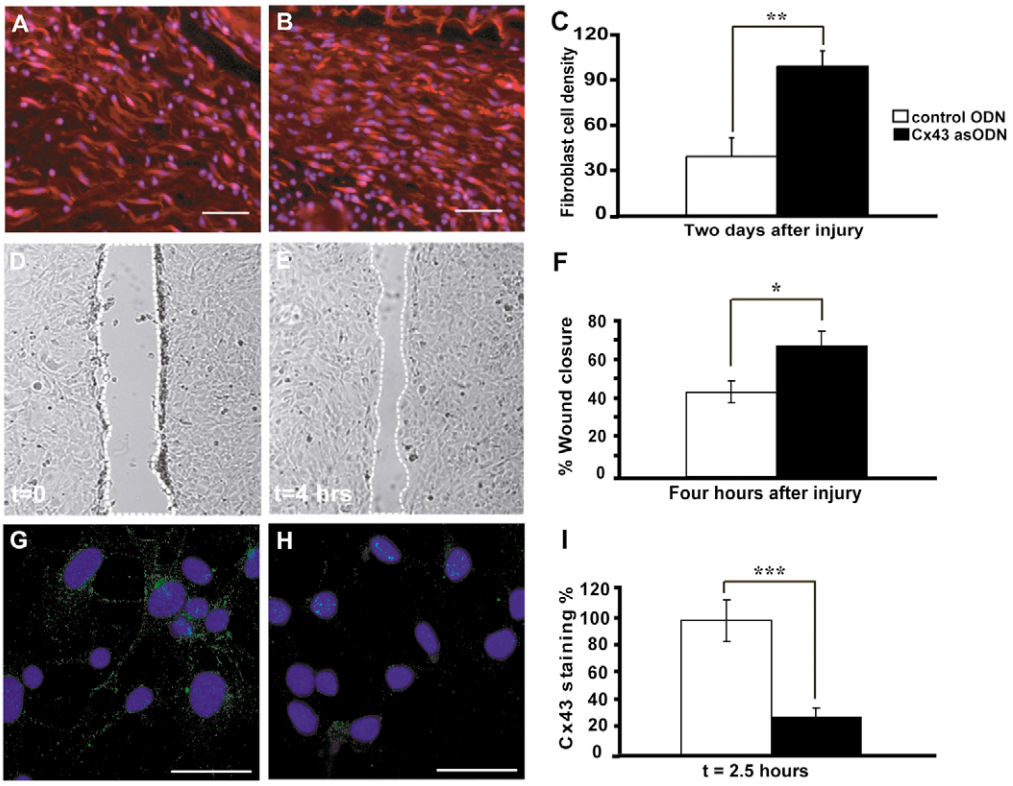

Fig. 7. Granulation tissue formation and fibroblast migration. (A,B) Fibroblast-like cell recruitment into skin wounds treated with control sODN (A) and Cx43-asODN (B), analyzed using TRITC-phalloidin and DAPI nuclear staining on day 2. (C) Number of fibroblast-like cells at each wound site per field of view for wounds treated with control sODN (white bars, n=5) or Cx43-asODN (black bars, n=5). (D-E) Images of wounds in fibroblast cultures at (D) the time of wounding and (E) 4 hours after wounding. (F) Wound-healing assay of fibroblast migration shows that migration is significantly faster after treatment with Cx43-asODNs. (G,H) Staining of fibroblasts for Cx43 in cultures treated with (G) control and (H) Cx43-asODN after 2.5 hours. (I) Quantification of Cx43 expression 2.5 hours after Cx43-asODN treatment, expressed as a percentage of control (n=8 per time point). Data are expressed as the mean ± s.e.m.; *P<0.02, **P<0.01, ***P<0.0001. Bars, 50 μm. For a high-resolution figure, please see the online version of this article.

many key events in the wound healing process: it is a potent immunosuppressive (Wahl, 1992); it can promote fibroblast migration and proliferation (Postlethwaite et al., 1987); enhance wound contraction (Beck et al., 1991; Liu et al., 2001); enhance granulation tissue formation through α-SMA in myofibroblasts (Desmouliere et al., 1993), enhance collagen synthesis and deposition (Shah et al., 1994), stimulate angiogenesis (Roberts et al., 1986) and promote re-epithelialization (Chesnoy et al., 2003). There remains a good deal of confusion associated with the effect TGF-β1 has when applied directly to the wound, different results being obtained depending on dosage and wounding model (Hebda et al., 1988; Mustoe et al., 1991; Garlick and Taichman, 1994). However, transgenic mice that overexpress TGF-β1 show a better quality of wound healing with reduced scar formation (Shah et al., 1999).

The elevated levels of TGF-β1 on day 2 appear to be mainly in the elongated fibroblast-like cells at the edge of the wound and in the keratinocytes at the edge of the wound. This ties in well with the previously-described effects of TGF-β1 on enhanced proliferation and migration (Postlethwaite et al., 1987), both of which we see in the early stages of tissue repair. Indeed, the TGF-β1 elevation may be one of the factors that, under these conditions, contribute to the promotion of healing, increasing the rate of proliferation and migration of fibroblasts and enhancing collagen synthesis.

Both, the active downregulation of Cx43 protein as well as TGF-β1 activate Col1α1 expression (Cutroneo, 2003; Waggett et al., 2006). Therefore, the enhanced Col1α1 expression and collagen deposition could be related to the increased expression of TGF-β1 at day 2, to the downregulation of Cx43 protein or both.

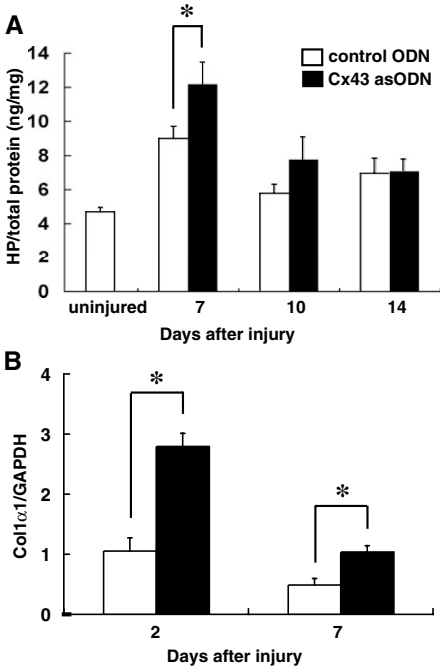

Fig. 8. Collagen expression in the wound site. (A) Collagen content was assessed by quantitatively measuring the hydroxyproline (HP) content on days 7, 10 and 14 after wounding at wound sites treated with control sODN (white bars) and Cx43-asODN (black bars) and in uninjured skin (n=5). Data are expressed as the mean ± s.e.m. P<0.05. (B) Real-time PCR analysis of the expression of mRNA on days 2 and 7 (n=5 for each) for Col1α1 at wound sites treated with control sODN (white bars) and Cx43-asODN (black bars). Data are expressed as the mean ± s.e.m.; *P<0.05.

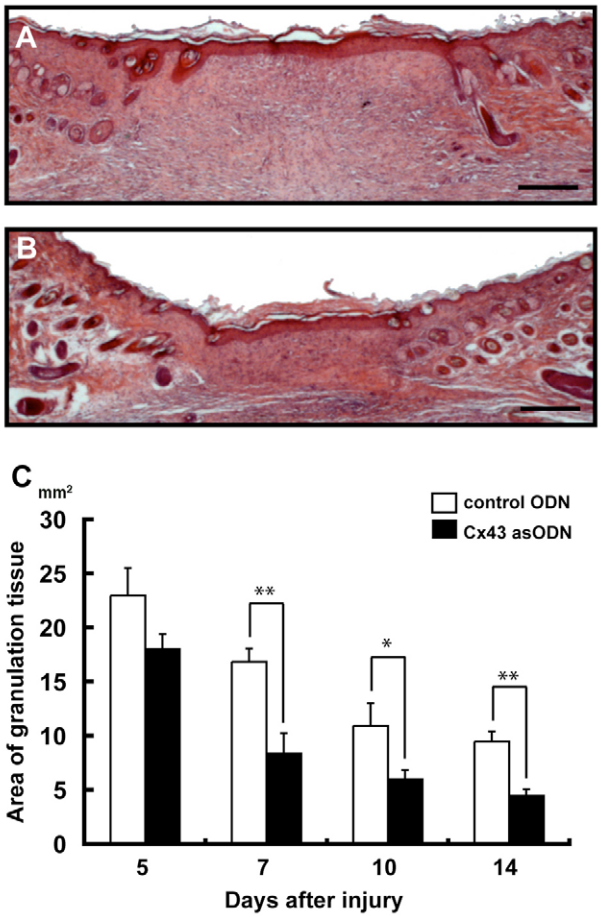

Fig. 9. Granulation tissue contraction. (A,B) H and E staining of 14-days-old wound granulation tissue in wounds treated with control sODN (A) and asODN (B). (C) Area of granulation tissue after treatment with control sODN (white bars) or Cx43-asODN (black bars) analyzed on day 5 (control, n=7; asODN, n=6), day 7 (control, n=5; asODN, n=5), day 10 (control, n=5; asODN, n=6), and day 14 (control, n=5; asODN, n=6). Granulation tissue area measurements at day 5 already showed a slightly smaller area after treatment but the reduction became significant on days 7, 10 and 14 (*P<0.05, **P<0.01). Data are expressed as the mean ± s.e.m. Bars, 1 mm.

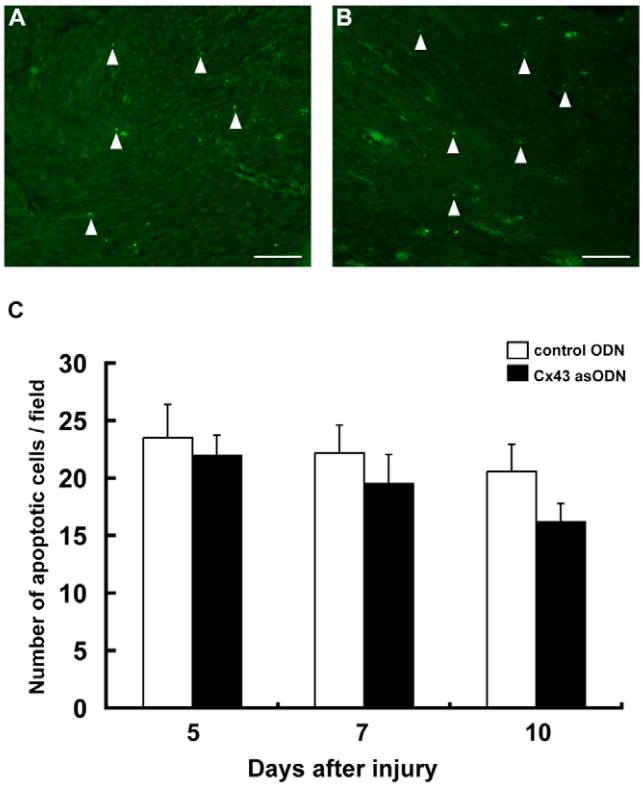

Fig. 10. Apoptosis. (A, B) TUNEL staining of granulation tissue in (A) control sODN and (B) Cx43-asODN-treated wounds on day 7. Apoptotic cells appear as bright green spots, some of which have been highlighted with arrowheads. (C) Numbers of apoptotic cells per field of view on days 5, 7 and 10 (n=6 for each) in wound sites treated with control sODN (white bars) and Cx43-asODN (black bars). Data are expressed as the mean ± s.e.m. Bars, 50 μm. For a high-resolution figure, please see the online version of this article.

Although TGF-β1 has been suggested to suppress inflammation, it is unlikely to be the main factor leading to the reduced inflammation we observe, because that is already evident on day 1 – before the TGF-β1 becomes elevated. Similarly, whereas TGF-β1 has been shown to promote angiogenesis and granulation-tissue maturation at later stages of the wound-healing process we see no elevation of TGF-β1 at these later time points; therefore, other factors must promote the enhanced maturation of granulation tissue.

Migration and proliferation

In this study we show enhanced migration of fibroblasts into the wound site and faster re-epithelialisation following Cx43-asODN treatment, indicating that Cx43 plays an important role in modulating cell movement. Contradictory results have been reported on the role of Cx43 in cell migration. Li and colleagues reported that in embryonic development, Cx43-deficient proepicardial cells migrated faster than those expressing Cx43 (Li et al., 2002). By contrast, the same group previously reported that Cx43-deficient neural crest cells showed decreased rates of migration (Huang et al., 1998). This latter finding is consistent with slowed rates of migration of retinal neuroepithelial cells that have had communication perturbed or Cx43 expression diminished (Pearson et al., 2005). These differences in the effects of communication on migration may perhaps reflect the different cell types involved and whether the cells migrate independently or in a communicating group.

Faster re-epithelialization and an enhanced rate of granulation tissue formation could also be attributed to the enhanced proliferation in the asODN-treated group, which we find in nascent epidermis and granulation tissue at both 2 days and 7 days after wounding. As with migration rates, there are mixed reports relating Cx43 expression and proliferation. Cx43-deficient proepicardial cell proliferation is increased, but this is not seen Cx43-deficient cardiac neural crest cells or in the developing neural retina treated with Cx43-asODNs where proliferation is reduced (Huang et al., 1998; Becker and Mobbs, 1999; Li et al., 2002). We show that, reducing Cx43 expression with asODNs in a fibroblast wound healing assay significantly accelerates their rate of migration. The Cx43 protein downregulation may therefore aid the faster re-

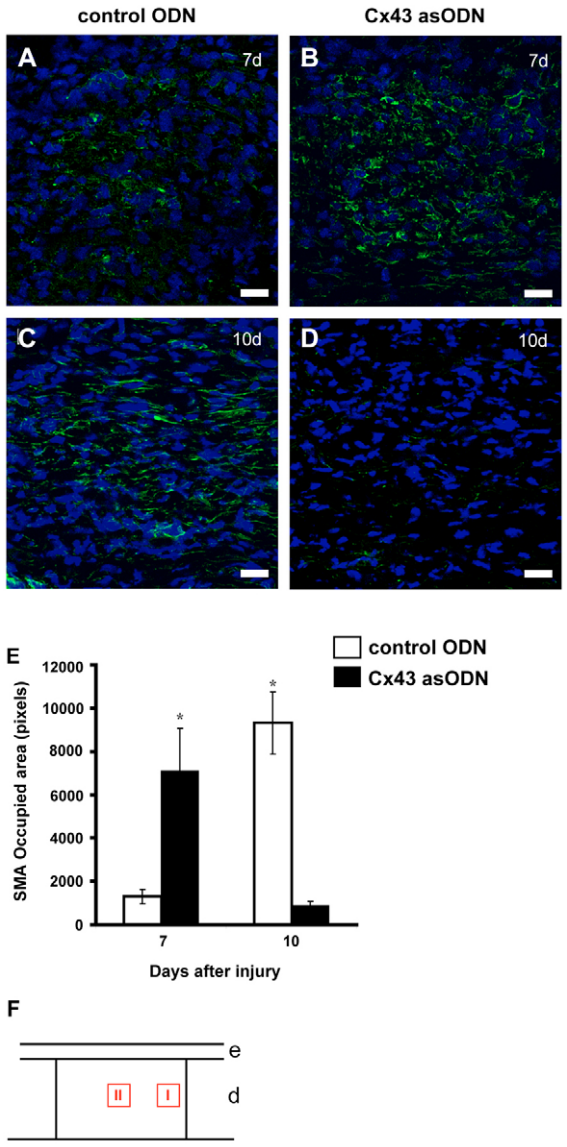

Fig. 11. Myofibroblast maturation. (A-D) anti-αSMA antibody staining (green) with bis-benzimide nuclear staining (blue) of (A,B) the edge of the granulation tissue in a 7 day wound and (C,D) the center of the granulation tissue in a 10 day wound. (E) Quantification of staining levels showed significantly more α-SMA staining in wounds treated with Cx43-asODN than with control sODN at 7 days (P=0.004) indicating earlier maturation and differentiation of myofibroblasts. This more advanced maturation was still present at 10 days when most of the α-SMA staining and myofibroblasts were lost in wounds treated with Cx43-asODN, but staining was still very strong in control wounds (P=0.000002). (F) Illustration of sites imaged in the granulation tissue. Zone I (A,B) zone II (C,D). e, epidermis; d, dermis. Data are expressed as the mean ± s.e.m. Bars, 25 μm. For a high-resolution figure, please see the online version of this article.

epithelialization and fibroblast migration into granulation tissue that we see. Alternatively the influence may come from the elevated levels of TGF-β1 on day 2 in Cx43-asODN-treated wounds, which has been suggested to enhance cell proliferation and increase rates of fibroblast migration, or perhaps a combination of both.

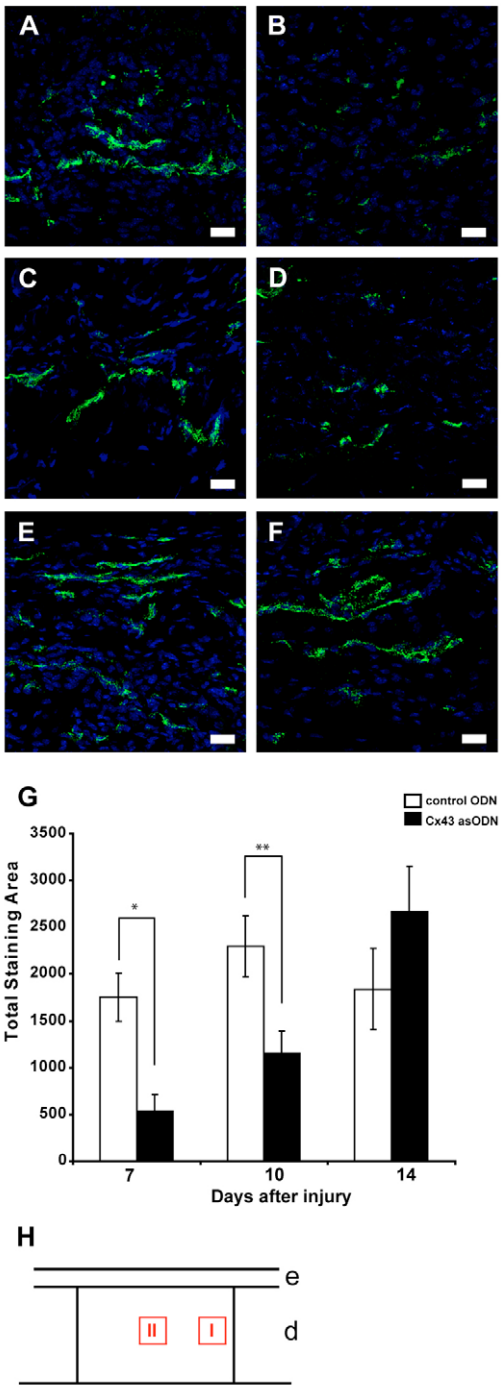

Fig. 12. Angiogenesis. (A-F) von Willebrand factor staining of nacent blood vessels granulation tissue (green) with bis-benzimide nuclear stain (blue) at 7 days (A,B), 10 days (C,D) and 14 days (E,F) after wounding. In Cx43-asODN-treated wounds (B,D,F) blood vessels were more pervasive at early time points (7 days, B; 10 days, D) but considerably finer than those of controls (A,C,E) resulting in significantly reduced staining compared with controls (7 days *P=0.0019; 10 days **P=0.015). By 14 days, blood vessels had increased in size in the asODN group and were a similar size to those of controls (G). (H) Illustration of sites imaged in the granulation tissue. Zone I (A,B) zone II (C-E). e, epidermis; d, dermis. Per treatment and time point six to eight animals were used. Data are expressed as the mean ± s.e.m. Bars, 25 μm. For a high-resolution figure, please see the online version of this article.

Angiogenesis

Angiogenesis is another central feature of granulation tissue maturation, involving invasion, expansion and then remodeling. Blood vessels growing into granulation tissue of Cx43-asODN-treated wounds were much finer and more advanced than those of the controls, entering the granulation tissue on day 5 and ramifying throughout the granulation tissue by day 7, when blood vessels were only seen at the edges of control granulation tissue. Interestingly, blood vessels in control wounds were thicker at these early stages and so gave a significantly greater area of staining at both 7 and 10 days. By 14 days the blood vessels in treated wounds had developed to a greater size and appeared to be very similar to controls. Cx43 is known to be involved in coronary vasculogenesis and angiogenesis (Walker et al., 2005). However, the observation that Cx43 protein levels were similar in control wounds and Cx43-asODN-treated wounds by day 7 after injury suggests that, at this stage, angiogenesis in Cx43-asODN-treated wounds had probably been indirectly influenced by the antisense-mediated changes that we saw at early stages. It is possible that angiogenesis is promoted by the early elevation in TGF-β1, because this growth factor has been reported to promote angiogenesis (Roberts et al., 1986); however, the time frames for this do not match.

In summary, this study analyzes the cell biology downstream of Cx43 protein reduction at wound sites, which strongly influences very early events in wound healing. In particular, it limits the extent of the inflammatory response and advances the onset and rate of re-epithelialization. There is an enhanced rate of granulation tissue formation, maturation and contraction. This approach clearly offers the potential for new therapies for improving wound healing in a variety of clinical situations.

Materials and Methods

Wound model and ODN treatment

Male, 8-week-old ICR mice were used in the experiments. All experiments were carried out at UCL according to UK Home Office regulations. Mice were anesthetized by halothane inhalation. Four full-thickness excisional wounds were made on the shaved back on either side of the dorsal midline with a 6-mm biopsy punch (Kai Industries). To each pair of wounds a single 50-μl topical application of 1 μM Cx43-asODN (Sigma-Genosys) in 30% Pluronic F-127 gel (Sigma-Aldrich) chilled on ice was made to one wound, and of 1 μM sense control sODNs was made to the other. Cx43-asODN application results in a significant knockdown of Cx43 protein at the site of delivery within 2 hours (Becker et al., 1999; McGonnell et al., 2001; Qiu et al., 2003). In some series of experiments, wounds and their surrounding area, including the scab and epithelial margins, were harvested with an 8-mm biopsy punch (Kai Industries). A minimum of eight mice were used for each time point examined.

Histology and immunostaining

Wound tissues were fixed in 4% formaldehyde buffered with PBS, and embedded in paraffin. Sections (6 μm thick) were stained with hematoxylin-eosin or analyzed immunohistochemically. Measurement of granulation tissue area in hematoxylin-eosin-stained tissue was performed using Improvision Openlab™ 4.0.2 software (Improvision). For immunohistochemistry, deparaffinized sections were treated with endogenous peroxidase blocking reagent (Dako Cytomation A/S) and proteinase K (Dako Cytomation A/S) for 20 minutes and 6 minutes at room temperature, respectively. They were then incubated with rabbit anti-myeloperoxidase (MPO) polyclonal antibody (NeoMarkers) diluted 1:200, rat anti-mouse F4/80 monoclonal antibody (mAb) against the marker of macrophage maturation and activation BM8 (Abcom Limited) diluted 1:400, rat anti-mouse CD31 (platelet endothelial cell adhesion molecule 1, PECAM-1) mAb (PharMingen) or rabbit anti-mouse TGF-β1 polyclonal antibody (Santa Cruz Biotechnology, Inc) 1:200 overnight at 4°C after blocking with 15% skimmed milk for 1 hour at room temperature. Some sections were reacted with phalloidin-tetramethylrhodamine B isothiocyanate (Sigma-Aldrich) diluted 1:500 for 1 hour at room temperature. Sections incubated with anti-MPO antibody and anti TGF-β1 antibody were stained with EnVision+™ (Dako Cytomation A/S) to enhance the signal. Sections incubated with anti-F4/80 and anti-CD31 antibodies were stained with biotinylated rabbit anti-rat immunoglobulin (Dako Cytomation A/S), 1:200 for 1 hour at 37°C. The signal was enhanced using the Catalyzed Signal Amplification System® (Dako Cytomation A/S). Counterstaining was performed with Methyl Green (Dako Cytomation A/S) followed by MPO-, TGF-β1-, F4/80- or CD31-staining, or with 4′,6-diamidino-2-phenylindole (DAPI) followed by phalloidin staining.

Immunostaining for Cx43, blood vessels or α smooth muscle actin (αSMA) was carried out on cryostat sections fixed in acetone at 4°C for 5 minutes prior to blocking for 45 minutes. Incubation for 1 hour with primary antibodies against: rabbit anti-Cx43 (Sigma) 1:3000; isoLectinB-FITC 1:2000; von Willebrand Factor (anti-rabbit, Dako) 1:400; anti-αSMA (Sigma) 1:400 at room temperature. Sections were washed and incubated for 1 hour with FITC-conjugated anti-rabbit IgG antibody (Dako) 1:200 at room temperature, followed by three washes for 5 minutes in PBS, in some cases with 1 μM bis-benzimide (Sigma) as a nuclear counter-stain, and mounted in Citifluor (Citifluor, London, UK). Sections were imaged by confocal microscopy; all parameters were kept the same to allow direct comparison of digital images.

TUNEL staining

Paraffin sections were de-waxed and treated with proteinase K (Dako Cytomation A/S) for 5 minutes at room temperature, and then stained using the In Situ Cell Death Detection Kit (Roche) according to the manufacturer's instructions. Counterstaining was performed with DAPI. TUNEL-stained sections were imaged and positive cells were counted in the granulation tissue of three random fields at the two sides and the center of each wound (each field was 0.332 mm^2).

Detection of proliferating cells by labeling with BrdU

Selected mice were injected intraperitoneally with 1 ml of BrdU (Sigma) in PBS (1 mg/ml) 2 hours before harvesting on days 1, 2 and 7. Tissues were fixed in 4% formaldehyde and embedded in paraffin. Deparaffinized sections (6 μm thick) were treated with a HistoMouse™-Plus Kit (ZYMED Laboratories, Inc.) to reduce background signals. Sections were stained with BrdU Detection Kit (BD Bioscience Pharmingen). Counterstaining was with Methyl Green (Dako Cytomation A/S).

Measurement of neutrophils, macrophages, fibroblasts, BrdU-positive cells and angiogenesis

A treatment-blinded observer counted MPO-positive neutrophils and F4/80-positive macrophages in the wound bed (defined as the area surrounded by unwounded skin, fascia, regenerated epidermis and eschar) in three random high-power fields of 0.332 mm^2. BrdU-positive cells in the wound margin and the nascent epidermis regions of each immunohistochemically stained section were counted as described previously, and are given as the number per 100 μm of epidermis (Mori et al., 2004). The number of fibroblast-like cells (phalloidin-positive cells with spindle-shape body) at the wound margin were counted (each field was 0.332 mm^2). The neovascularization was followed using von Wildebrand factor fluorescent staining of endothelial cells at days 5, 7, 10 and 14 after wounding. Myofibroblasts were identified by anti-αSMA staining. For quantification of both fluorescent stains, single-section images from comparable zones from a minimum six animals per time point were taken on a confocal microscope. All parameters of image acquisition were kept the same to allow comparison. Images were made binary at a standard threshold and positive pixels were counted using Image J (NIH Image).

Hydroxyproline analysis

The collagen content of the wound area was assessed by determining the amount of hydroxyproline (HP), a major component of collagen (Woessner, 1961). Samples were homogenized in 1 ml of T-PER® tissue protein extraction reagent (PIERCE Biotechnology Inc.) including Halt™ protease inhibitor cocktail, EDTA-free (PIERCE Biotechnology Inc.), centrifuged at 15,000 ***g*** for 20 minutes at 4°C to remove the debris. Concentrations of protein were measured using a BCA™ protein assay kit (PIERCE Biotechnology Inc.), and the amounts of HP were determined with Sircol™ soluble collagen assay kit (Biocolor Ltd). The data were expressed as amounts of HP per total protein (ng/μg) for each sample.

Cell culture

Swiss 3T3 fibroblasts were grown in Dulbecco's modified Eagle's medium (DMEM; Gibco) supplemented with 10% fetal calf serum (Labtech) and 1% penicillin-streptomycin solution (Sigma, Poole) in a 5% CO_2 incubator at 37°C unless otherwise stated. Cells were passaged and used at passages six to ten at a confluency of approximately 90%. Cells were plated on 13-mm glass coverslips in 24-well dishes (Nunc) with 4×10^5 to 5×10^5 cells per well, containing 1 ml of medium. Cells reached confluency after 72 hours and were then considered ready for experimentation.

Cell migration assay by wounding

Wounding was performed by drawing a microelectrode across a confluent coverslip, producing a lesion of standard width (Lampugani, 1999). Phase-contrast images were acquired at ×5 magnification on a Zeiss inverted microscope with an incubation chamber at 37° and 5% CO_2. An image of a defined area at the edge of a coverslip was taken immediately after wounding and a further image was taken of the same area 4 hours later, a time at which migration was clearly seen to have taken place (Fig. 7D,E). A minimum of eight coverslips were imaged in each group.

Migration was quantified by measuring the change in wound area (pixels) using Image J software (NIH).

To knock down Cx43 expression in the fibroblasts the serum-supplemented DMEM was replaced for 2 hours with serum-free DMEM containing either 20 μM asODNs or 20 μM control sODNs before changing back to serum-supplemented DMEM. The wounding assay was then carried out as above.

Isolation of RNA and quantitative gene expression analysis by RT-PCR

Total RNA was extracted from skin wound samples using TRIzol reagent (Invitrogen). Ten micrograms of total RNA was reverse-transcribed into cDNA using the SuperScript First-Strand Synthesis System for RT-PCR (Invitrogen). Gene-specific primers and probe were obtained as TaqMan® gene expression assays (Applied Biosystems) for Cx43, Ccl2, Colα1, TNFα and TGFβ1. The enzyme and buffer system was purchased as TaqMan® universal PCR master Mix (Applied Biosystemes). Each sample was analyzed in duplicate. Amplification and real-time detection was performed in the DNA engine Opticon®2 (MJ Research Inc.). Expression of target genes was compared with GAPDH expression.

Statistical analysis

Statistical differences were determined using the unpaired Student's *t*-test or the Mann Whitney *U* test as appropriate. All data are presented as the mean ± s.e.m. Criterion levels for the individual tests are given in Results.

We owe thanks to the Uehara Memorial Foundation, the Nakatomi Foundation and the Japan Society for the Promotion of Science postdoctoral fellowships for research abroad (RM); to The Wellcome Trust and the BBSRC for funding; to Brian Stramer (Bristol) and Kazuya Ikematsu (Nagasaki University, Japan) for assistance with fibroblast analysis and analysis of real-time PCR data, respectively; to Deborah Martin and Debra Ford (Bristol) and Chris Thrasivoulou (UCL) for histological assistance; to Jeremy Cook (UCL) for his comments on the manuscript.

References

Bannerman, P., Nichols, W., Puhalla, S., Oliver, T., Berman, M. and Pleasure, D. (2000). Early migratory rat neural crest cells express functional gap junctions: evidence that neural crest cell survival requires gap junction function. *J. Neurosci. Res.* **61**, 605-615.

Beck, L. S., Deguzman, L., Lee, W. P., Xu, Y., McFatride, L. and Amento, E. P. (1991). TGF-β1 accelerates wound healing: reversal of steroid-impaired healing in rats and rabbits. *Growth Factors* **5**, 295-304.

Becker, D. L. and Mobbs, P. (1999). Connexin α1 and cell proliferation in the developing chick retina. *Exp. Neurology* **156**, 326-332.

Becker, D. L., McGonnell, I., Makarenkova, H. P., Patel, K., Tickle, C., Lorimer, J. and Green, C. R. (1999). Roles for alpha 1 connexin in morphogenesis of chick embryos revealed using a novel antisense approach. *Dev. Genet.* **24**, 33-42.

Bowman, N. N., Donahue, H. J. and Ehrlich, H. P. (1998). Gap junctional intercellular communication contributes to the contraction of rat osteoblast populated collagen lattices. *J. Bone Miner. Res.* **13**, 1700-1706.

Chesnoy, S., Lee, P. Y. and Huang, L. (2003). Intradermal injection of transforming growth factor-beta1 gene enhances wound healing in genetically diabetic mice. Pharm. Res. **20**, 345-350.

Coutinho, P., Qiu, C., Frank, S., Tamber, K. and Becker, D. L. (2003). Key events in the wound healing process correlate with changes in connexin expression. *Cell Biol. Int.* **27**, 525-541.

Coutinho, P., Qiu, C., Frank, S., Wang, C. M., Brown, T., Green, C. R. and Becker, D. L. (2005). Limiting burn extension by transient inhibition of Connexin43 expression at the site of injury. *Br. J. Plast. Surg.* **58**, 658-667.

Cronin, M., Anderson, P., Green, C. R. and Becker, D. L. (2006). Antisense delivery and protein knockdown within the intact central nervous system *Front. Biosci.* **11**, 2967-2975.

Cutroneo, K. R. (2003). How is Type I procollagen synthesis regulated at the gene level during tissue fibrosis. *J. Cell Biochem.* **90**, 1-5.

Desmouliere, A., Geinoz, A., Gabbiani, F. and Gabbiani, G. (1993). Transforming growth factor-beta 1 induces alpha-smooth muscle actin expression in granulation tissue myofibroblasts and in quiescent and growing cultured fibroblasts. *J. Cell Biol.* **122**, 103-111.

Dovi, J. V., He, L. K. and DiPietro, L. A. (2003). Accelerated wound closure in neutrophil-depleted mice. *J. Leukoc. Biol.* **73**, 448-455.

Ehrlich, H. P. and Rittenberg, T. (2000). Differences in the mechanism for high- versus moderate-density fibroblast-populated collagen lattice contraction. *J. Cell Physiol.* **185**, 432-439.

Gaietta, G., Deerinck, T. J., Adams, S. R., Bouwer, J., Tour, O., Laird, D. W., Sosinsky, G. E., Tsien, R. Y. and Ellisman, M. H. (2002). Multicolor and electron microscopic imaging of connexin trafficking. *Science* **296**, 503-507.

Garlick, J. A. and Taichman, L. B. (1994). Effect of TGF-beta 1 on re-epithelialization of human keratinocytes in vitro: an organotypic model. *J. Invest. Dermatol.* **103**, 554-559.

Goliger, J. A. and Paul, D. L. (1995). Wounding alters epidermal connexin expression and gap junction-mediated intercellular communication. *Mol. Biol. Cell* **6**, 1491-1501.

Grose, R. and Werner, S. (2004). Wound-healing studies in transgenic and knockout mice. *Mol. Biotechnol.* **28**, 147-166.

Hebda, P. A. (1988). Stimulatory effects of transforming growth factor-beta and epidermal growth factor on epidermal cell outgrowth from porcine skin explant cultures. *J. Invest. Dermatol.* **91**, 440-445.

Huang, G. Y., Cooper, E. S., Waldo, K., Kirby, M. L., Gilula, N. B. and Lo, C. W. (1998). Gap junction-mediated cell-cell communication modulates mouse neural crest migration. *J. Cell Biol.* **143**, 1725-1734.

Kwak, B. R., Pepper, M. S., Gros, D. B. and Meda, P. (2001). Inhibition of endothelial wound repair by dominant negative connexin inhibitors. *Mol. Biol. Cell* **12**, 831-845.

Laird, D. W., Puranam, K. L. and Revel, J. P. (1991). Turnover and phosphorylation dynamics of connexin43 gap junction protein in cultured cardiac myocytes. *Biochem. J.* **273**, 67-72.

Lampugnani, M. G. (1999). Cell migration into a wounded area in vitro. *Methods Mol Biol.* **96**, 177-182.

Li, W. E., Waldo, K., Linask, K. L., Chen, T., Wessels, A., Parmacek, M. S., Kirby, M. L. and Lo, C. W. (2002). An essential role for connexin43 gap junctions in mouse coronary artery development. *Development* **129**, 2031-2042.

Liu, X. D., Umino, T., Ertl, R., Veys, T., Skold, C. M., Takigawa, K., Romberger, D. J., Spurzem, J. R., Zhu, Y. K., Kohyama, T. et al. (2001). Persistence of TGF-beta1 induction of increased fibroblast contractility. *In Vitro Cell Dev. Biol. Anim.* **37**, 193-201.

Lucke, T., Choudhry, R., Thom, R., Selmer, I. S., Burden, A. D. and Hodgins, M. B. (1999). Upregulation of connexin 26 is a feature of keratinocyte differentiation in hyperproliferative epidermis, vaginal epithelium, and buccal epithelium. *J. Invest. Dermatol.* **112**, 354-361.

Martin, P. (1997). Wound healing – aiming for perfect skin regeneration. *Science* **276**, 75-81.

Martin, P. and Leibovich, S. J. (2005). Inflammatory cells during wound repair: the good, the bad and the ugly. *Trends Cell Biol.* **15**, 599-607

Martin, P., D'Souza, D., Martin, J., Grose, R., Cooper, L., Maki, R. and McKercher, S. R. (2003). Wound healing in the PU.1 null mouse–tissue repair is not dependent on inflammatory cells. *Curr. Biol.* **13**, 1122-1128.

McGonnell, I. M., Green, C. R., Tickle, C. and Becker, D. L. (2001). Connexin43 gap junction protein plays an essential role in morphogenesis of the embryonic chick face. *Dev. Dyn.* **222**, 420-438.

Mori, R., Kondo, T., Nishie, T., Ohshima, T. and Asano, M. (2004). Impairment of skin wound healing in beta-1,4-galactosyltransferase-deficient mice with reduced leukocyte recruitment. *Am. J. Pathol.* **164**, 1303-1314.

Mustoe, T. A., Pierce, G. F., Morishima, C. and Deuel, T. F. (1991). Growth factor-induced acceleration of tissue repair through direct and inductive activities in a rabbit dermal ulcer model. *J. Clin. Invest.* **87**, 694-703.

Oviedo-Orta, E. and Evans, W. H. (2004). Gap junctions and connexin-mediated communication in the immune system. *Biochim. Biophys. Acta* **1662**, 102-112.

Oviedo-Orta, E., Hoy, T. and Evans, W. H. (2000). Intercellular communication in the immune system: differential expression of connexin40 and 43, and perturbation of gap junction channel functions in peripheral blood and tonsil human lymphocyte subpopulations. *Immunology* **99**, 578-590.

Oviedo-Orta, E., Gasque, P. and Evans, W. H. (2001). Immunoglobulin and cytokine expression in mixed lymphocyte cultures is reduced by disruption of gap junction intercellular communication. *FASEB J.* **15**, 768-774.

Pearson, R., Luneborg, N., Becker, D. L. and Mobbs, P. (2005). Gap junctions modulate interkinetic nuclear migration in retinal progenitor cells. *J. Neurosci.* **25**, 10803-10814.

Postlethwaite, A. E., Keski-Oja, J., Moses, H. L. and Kang, A. H. (1987). Stimulation of the chemotactic migration of human fibroblasts by transforming growth factor beta. *J. Exp. Med.* **165**, 251-256.

Qiu, C., Coutinho, P., Frank, S., Franke, S., Law, L. Y., Martin, P., Green, C. R. and Becker, D. L. (2003). Targeting connexin43 expression accelerates the rate of wound repair. *Curr. Biol.* **13**, 1697-1703.

Roberts, A. B., Sporn, M. B., Assoian, R. K., Smith, J. M., Roche, N. S., Wakefield, L. M., Heine, U. I., Liotta, L. A., Falanga, V., Kehrl, J. H. et al. (1986). Transforming growth factor type beta: rapid induction of fibrosis and angiogenesis in vivo and stimulation of collagen formation in vitro. *Proc. Natl. Acad. Sci. USA* **83**, 4167-4171.

Rossi, D. and Zlotnik, A. (2000). The biology of chemokines and their receptors. *Annu Rev Immunol* **18**, 217-242.

Shah, M., Foreman, D. M. and Ferguson, M. W. (1994). Neutralising antibody to TGF-beta 1,2 reduces cutaneous scarring in adult rodents. *J. Cell Sci.* **107**, 1137-1157.

Shah, M., Revis, D., Herrick, S., Baillie, R., Thorgeirson, S., Ferguson, M. and Roberts, A. (1999). Role of elevated plasma transforming growth factor-beta1 levels in wound healing. *Am. J. Pathol.* **154**, 1115-1124.

Waggett, A. D., Benjamin, M. and Ralphs, J. R. (2006). Connexin 32 and 43 gap junctions differentially modulate tenocyte response to cyclic mechanical load. *Eur. J. Cell Biol.* **85,** 1145-1154.

Wahl, S. M. (1992). Transforming growth factor beta (TGF-beta) in inflammation: a cause and a cure. *J. Clin. Immunol.* **12**, 61-74.

Walker, D. L., Vacha, S. J., Kirby, M. L. and Lo, C. W. (2005). Connexin43 deficiency causes dysregulation of coronary vasculogenesis. *Dev. Biol.* **284**, 479-498.

Wei, C. J., Xu, X. and Lo, C. W. (2004). Connexins and cell signaling in development and disease. *Annu. Rev. Cell. Dev. Biol.* **20**, 811-838.

Woessner, J. (1961). The determination of hydroxyproline in tissue and protein samples containing small proportions of the imino acid. *Arch. Biochem. Biophys.* **93**, 440-447.